Sea-Breeze Front Effects on Boundary-Layer Aerosols at a Tropical Coastal Station

K. KRISHNA MOORTHY, B. V. KRISHNA MURTHY, AND PRABHA R. NAIR

Space Physics Laboratory, Vikram Sarabhai Space Centre, Trivandrum, India

(Manuscript received 13 February 1992, in final form 31 August 1992)

ABSTRACT

The effects of sea breeze on optical depth, size distribution, and columnar loading of aerosols at the tropical coastal station of Trivandrum are studied. It has been observed that sea-breeze front activity results in a significant and short-lived enhancement in aerosol optical depth and columnar loading in contrast to the effects seen on normal sea-breeze days. Examination of the changes in columnar aerosol size distribution associated with sea-breeze activity revealed an enhancement of small-particle (size less than 0.28 μm) concentration. The aerosol size distributions deduced from optical depth measurements generally show a pronounced bimodal structure associated with the frontal activity.

1. Introduction

Studies on lake- and sea-breeze activity at coastal regions have shown occasional occurrences of sea-breeze front on sunny days preceded by cool nights. Such "fronts" are generally identified by a rather abrupt shift in the horizontal wind direction accompanied by a sharp increase in relative humidity and drop in temperature (e.g., Bornstein and Thompson 1981). They are also known to produce horizontal convergence and vertical updrafts in the boundary layer over the coastal land, leading to recycling of pollutants (Keen and Lyons 1978; Ogawa et al. 1986). The fronts, at times, are observed to penetrate inland as much as 30–40 km or more (Lyons and Olsson 1973; Simpson et al. 1977). The reverse phenomenon (land-breeze effect) of advection of cool land air over a warmer marine boundary layer causing convergence accumulation of aerosols and leading to production of haze has also been studied (Parvanov et al. 1988). Studies on such frontal activities are very important in pollution dispersion at coastal regions, since strong fronts can lead to recycling of pollutants in the boundary layer. Lyons and Olsson (1973) and Keen and Lyons (1978) have carried out extensive investigations on the response of shoreline smoke (industrial exhaust) to the lake breeze from Lake Michigan. We have investigated the effects of sea breeze on natural aerosols in a coastal environment in a tropical region far removed from any source of industrial pollution and present the results in this communication. The study has been conducted at Trivandrum (8.55°N, 76.9°E) situated at the southwest coast of India, during some clear (cloud free) days of February–March 1990 when sea-breeze activity was clearly discernible. The experimental site is a plain coastal land close to the sea level, characterized by fairly flat and sandy terrain. The experiments are conducted at approximately 500 m inland off the sea coast.

It is well known that sea breeze is a mesoscale meteorological phenomenon driven basically by the land–sea thermal contrast arising out of the different heat capacities of land and ocean. Its features are influenced also by the prevailing wind, surface heating, and frictional retardation over land. Studies at the coastal station, Trivandrum, by Narayanan (1967) have revealed that the period from November to April is generally favorable for sea-breeze activity. The diurnal variation of surface wind during this period is generally characterized by a land breeze (seaward flow) during the night and early morning hours (approximately 2100–0900 IST, corresponding to 82.5°E) and a sea breeze (landward flow) during the rest of the daytime and early nighttime. The land breeze is generally northerly or northeasterly, while the sea breeze is westerly or southwesterly. During the months from May to September the strong surface westerlies associated with the southwest monsoon completely mask the sea-breeze activity and a more or less continuous "sea wind" (westerly) prevails throughout this season (Narayanan 1967; Nair and Narayanan 1980). During periods when the prevailing winds are offshore, a convergence zone would form associated with the reversal of wind from offshore to onshore (onset of sea breeze) which may lead to the formation of a sea-breeze front with a sharp boundary (Hunt and Simpson 1982). These days are generally characterized by sharp changes in surface relative humidity RH and temperature T associated

Corresponding author address: Dr. B. V. Krishna Murthy, Space Physics Laboratory, Government of India, Vikram Sarabhai Space Centre, Trivandrum, India, 695 022.

with the onset of sea breeze (i.e., reversal of land breeze to sea breeze) and these are considered as "front" days in this study. The occurrence of such front days is found to be by far less numerous at Trivandrum, compared to the other days considered as "normal sea-breeze" days when the onset of sea breeze is gradual with no significant changes in RH and T (Prakash et al. 1992). Of the six days for which the effects on aerosols have been studied in the present investigation, four days correspond to the "front" days and two to "normal" days. All these six days had clear sky conditions, free from any visible clouds and synoptic-scale meteorological disturbances.

2. Experimental setup and analysis of data

The instrumental setup included (a) a passive multiwavelength solar radiometer (MWR) for estimating columnar aerosol optical depths at nine narrow spectral bands in the visible through near-infrared (Moorthy et al. 1989). The bands are centered at 400, 450, 500, 590, 700, 750, 800, 935, and 1025 nm with a full-width half-maximum bandwidth of 5 nm at each wavelength. The system has a field of view of less than 2°; (b) a set of tower-mounted instruments providing continuous measurement of surface-layer meteorological parameters, namely, wind (three components), temperature, and relative humidity (Prakash et al. 1992). These instruments are installed at three levels, namely, 5, 11, and 25 m above ground. Using the above instruments, observations were carried out on six days in February–March 1990, when sea-breeze activity was clearly discernible from the surface meteorological (MET) data.

Instantaneous optical depth τ has been evaluated for each of the MWR observations at each wavelength by constructing individual Langley plots using the mean zero airmass intercept evaluated separately for each wavelength following the Langley plot method (Shaw et al. 1973; Moorthy et al. 1989). From these τ values, aerosol optical depths τ_p have been deduced by subtracting the contributions due to molecular scattering and absorption by ozone and water vapor. The contributions due to molecular scattering and absorption by O_3 have been obtained using the relevant wavelength-dependent scattering and absorption cross sections and model profiles of neutral atmosphere and ozone for Trivandrum (Moorthy et al. 1989). Using the optical depths at 935 nm (peak of $\rho\sigma\tau$ absorption band of water vapor), along with those at 800 and 1025 nm (where the absorption due to water vapor is negligible), the columnar content of atmospheric water vapor has been estimated by employing the transmission function (Leckner 1978) and atmospheric models relevant for Trivandrum (Sasi and Sen Gupta 1979). Using these values of water vapor content, the optical depths due to absorption by water vapor at all the other wavelengths have been computed (Leckner 1978). These components of optical depths due to molecular scattering and absorption are subtracted from the optical depths τ at each wavelength to obtain the instantaneous aerosol optical depth τ_p. Thus on each observation day we have instantaneous values of aerosol optical depths τ_p at nine wavelengths 400, 450, 500, 590, 700, 750, 800, 935, and 1025 nm and these are examined for the study of the effects of sea-breeze activity. Since there are no major sources or sinks of aerosols for several kilometers around the observation site and since the time constants of upper-tropospheric and stratospheric aerosols are fairly long, the short-term temporal variations in measured τ_p can be attributed mainly to those arising from changes in the properties and loading of aerosols in the boundary layer over the observing station.

From the spectral aerosol optical depths, the height-integrated (columnar) size distributions of aerosols have been deduced by inverting the integral equation for optical depth,

$$\tau_p(\lambda) = \int_{r_a}^{r_b} \pi r^2 Q_{\text{ext}}(m, r, \lambda) N_c(r) dr, \qquad (1)$$

where $\tau_p(\lambda)$ is the aerosol optical depth at wavelength λ; Q_{ext} the Mie extinction efficiency factor which is a function of the particle radius r, λ and complex refractive index m; and $N_c(r)dr$ the columnar size distribution function of aerosols in the radii range r_a and r_b. The inversion of the above integral equation is carried out following the well-known constrained linear inversion technique using a Lagrange multiplier (King 1982). The details of the application of this technique to the MWR data at Trivandrum have been described elsewhere (Moorthy et al. 1991). Following the above technique, aerosol size distributions have been derived from the instantaneous τ_p values at specific times of interest. The columnar loading N_t of aerosols has been computed by numerically integrating the size distributions over the radii range r_a to r_b so that

$$N_t = \int_{r_a}^{r_b} N_c(r) dr. \qquad (2)$$

The columnar content of aerosols for three size intervals within the range r_a to r_b has also been estimated from the size distributions to examine the effects of sea-breeze activity on different particle size ranges.

The meteorological data used in the present study include the horizontal wind components (westerly component U and southerly component V), relative humidity RH, and temperature T recorded at 5-m level by the tower-mounted instruments. The data of higher levels (11 and 25 m) are not considered since they did not carry any signature distinct from that at the lower level as far as sea-breeze activity is concerned. From the U and V components the wind direction θ (measured clockwise with respect to north) and the sea-breeze component U_s, defined as the component of horizontal wind normal to the local coastline, has been

deduced. The local coastline is along 145°–325° azimuth and thus U_s is the wind component along 55°–235°. It is taken as positive for sea breeze (azimuth 55°) and as negative for land breeze (azimuth 235°). The time of reversal of U_s from negative to positive during the day has been considered as the time of onset of sea breeze.

3. Results

In the following we present the results corresponding to the six days of observations on a day-by-day basis.

a. 8 February 1990

The temporal variations of MET parameters shown in Fig. 1 indicate that this day is a normal sea-breeze day. (Wind directions with azimuth angle lying between 325° and 145° through 0° indicate the presence of a sea-breeze component whereas those between 145° and 325° indicate the presence of a land-breeze component.) Figure 1 clearly shows the presence of sea breeze right from 0745 IST onward, though weak. The RH initially dropped to approximately 45% at 0845 and subsequently increased gradually to reach 60% by about 1000 and remained steady from then onward. Temperature increased till 0830 and later remained steady. The temporal variations of aerosol optical depths on this day are shown in Fig. 2a at two representative wavelengths, 450 and 750 nm. The optical depths remained more or less steady during the interval from 0915 to 1200 IST except for some minor fluctuations. At other wavelengths too, τ_p showed similar temporal variations.

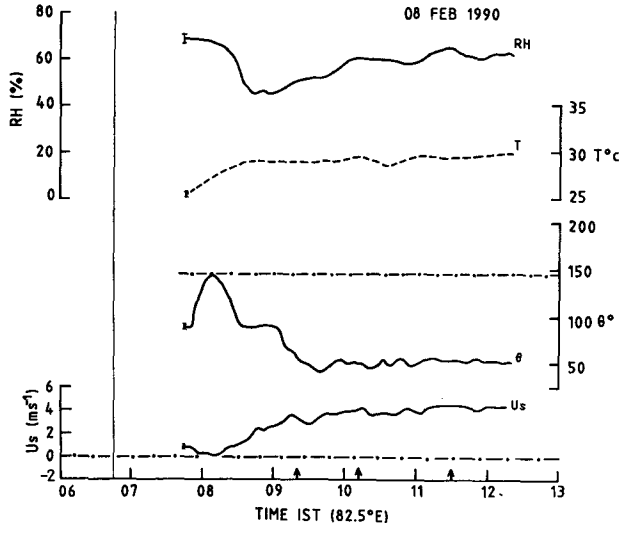

FIG. 1. Temporal variations of meteorological parameters (5 m above ground) for 8 February 1990. From bottom to top are plotted the sea-breeze component U_s, the wind direction θ, temperature T (°C), and the relative humidity RH (%). The dash–dot horizontal lines demarcate the land- and sea-breeze regimes. Error bars for each of the parameters are indicated by a vertical line at the beginning of the curves. A long vertical line on the X axis indicates the sunrise time. The arrow marks on the X axis indicate the times at which the aerosol size distributions have been estimated from τ_p values.

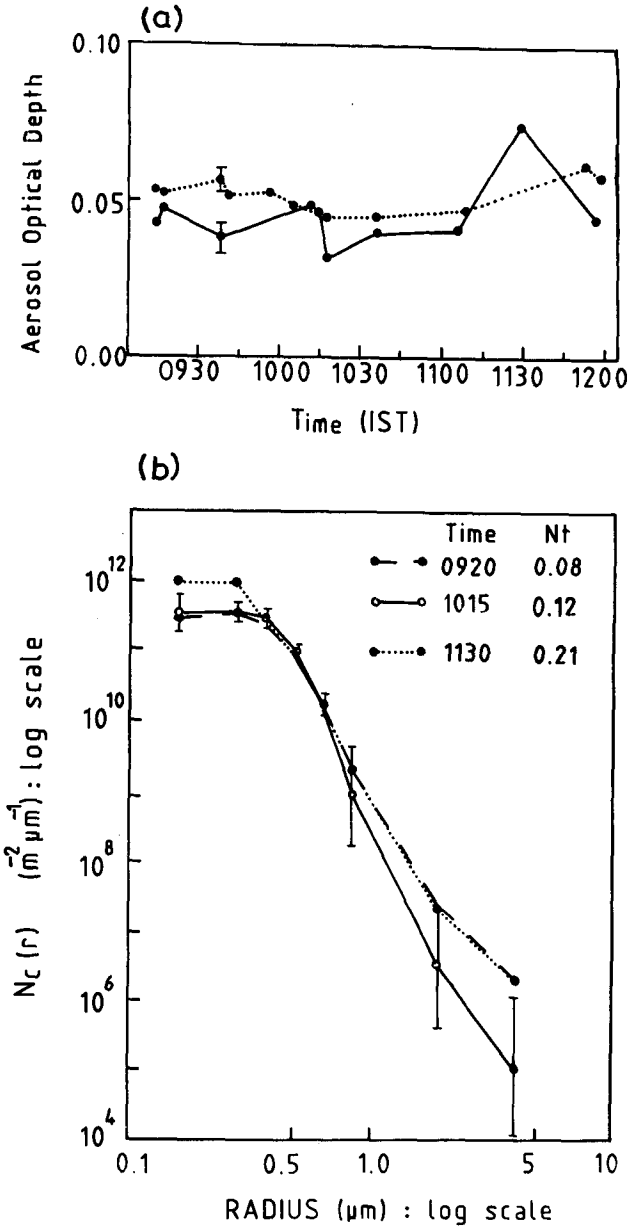

FIG. 2. (a) Temporal variations of aerosol optical depths at two representative wavelengths, 450 nm (continuous line) and 750 nm (dotted line), obtained from MWR data on 8 February 1990. The variations at other MWR wavelengths are not shown but are similar in nature. The vertical bars indicate the errors in τ_p. (b) Aerosol size distributions obtained by inverting the spectral optical depths. The time corresponding to each and the integrated columnar content N_t (10^{12} m^{-2}) are also given in the figure. The error bars are shown for the continuous line distribution only. For the other distributions also, these error bars are of similar magnitudes.

The size distributions (SDs) obtained from τ_p values at 0920, 1015, and 1130 IST are shown in Fig. 2b. These times are indicated in Fig. 1 using arrow marks on the abscissa. The three distributions are similar to each other and closely resemble modified Junge power-law distribution (McClatchy et al. 1972). The total aerosol content N_t (noted in Fig. 2b) shows a gradual increase with time. It is also seen that there is an increase in the concentration of particles with $r < 0.28$ μm at 1130 IST compared to the earlier times. The differences in the SDs at sizes greater than 1.0 μm are within the error bars.

b. 21 February 1990

Compared to 8 February 1990, the onset of sea breeze is much later on this day, occurring at 1036 IST as can be seen from Fig. 3. The change in wind direction toward land is quite rapid. However, the direction has not turned toward 55° azimuth but turned only to 100° azimuth. The land breeze was about 1.5 m s^{-1} prior to the reversal and sea breeze was about 4.5 to 5 m s^{-1} (after it stabilized) at approximately 1120. Relative humidity shows a decrease between 0915 and 1036 followed by a rapid increase. It recovers sharply to almost the same level that existed prior to the decrease, during the period 1036–1120 IST. Temperature shows an increase up to 1036 followed by steep decrease of 1°C. The rapid increase (decrease) of RH (T) occurs at the same time as the onset of sea breeze. Based on these rapid changes this day is considered as a "sea-breeze front" day in our study.

The aerosol optical depths at the two representative wavelengths 450 and 750 nm on this day are shown in Fig. 4a. It is seen from the figure that an abrupt increase in τ_p occurred at about 1048 IST, about 12 min after the onset of the front. An examination of the

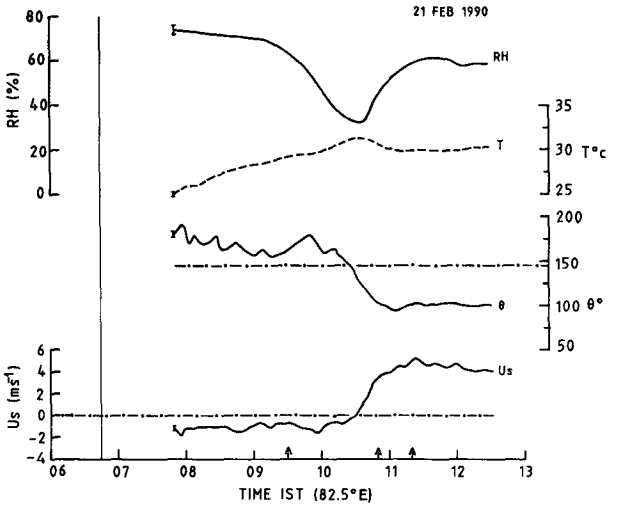

FIG. 3. Same as Fig. 1 but for 21 February 1990.

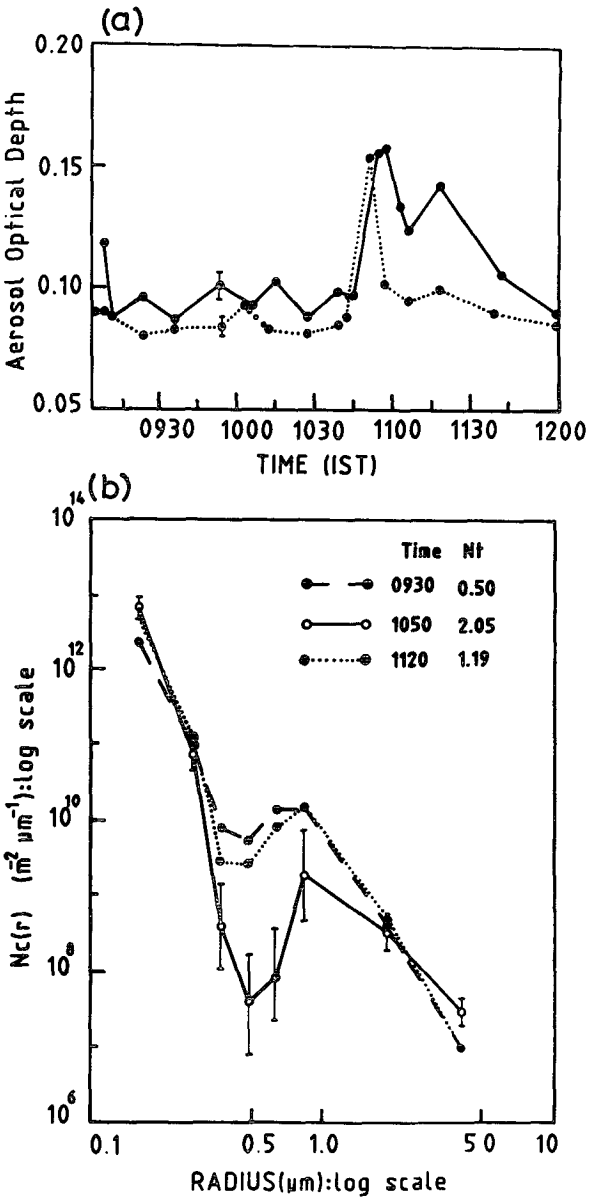

FIG. 4. Same as Fig. 2 but for 21 February 1990.

optical depths at all the other wavelengths also (not shown in Fig. 4a) revealed that τ_p reached its peak between 1044 and 1054 and then decreased to nearly the same values as existed during the land breeze. Figure 4b shows the SDs obtained from the optical depths at 0930, 1050, and 1120 IST corresponding to steady land breeze, peaking of τ_p associated with the front, and steady sea-breeze conditions, respectively. Unlike on 8 February, the distributions are bimodal, showing the presence of a secondary peak at the 0.8-μm size. The distribution at 1050 IST (corresponding to the time of occurrence of τ_p peak) shows an increase in the small-particle concentration (with radii <0.28 μm) and a very pronounced decrease in the concentration

with radii in the range of approximately 0.28 to 2.0 μm compared to the distribution corresponding to the land-breeze condition (0930 IST). By 1120 the distribution has almost recovered its original (0930) shape, especially at sizes greater than 0.28 μm.

c. 28 February 1990

This is also a front day as seen from the behavior of MET parameters shown in Fig. 5. The sea breeze had set in quite abruptly at 1013 IST on this day, but prior to that the wind fluctuated between landward and seaward directions from 0916 to 0958 IST. After 1016, the sea breeze remained more or less steady both in direction and magnitude. The final breeze direction and the values of U_s during the land-breeze and sea-breeze regimes are very much similar to those on 21 February. Relative humidity decreased prior to the onset of sea breeze; at the onset it showed an abrupt increase from 43% to 63% and the temperature dropped abruptly by 1°C.

The temporal variation of τ_p at 450 and 750 nm shown in Fig. 6a reveals again a remarkable increase in τ_p associated with the sea-breeze front, similar to the previous event. The increase in τ_p started at approximately 1018 IST, about 5 min later than the onset of the sea breeze, gradually reached its peak during 1036–1051 IST (considering all the wavelengths), and later decreased until about 1108 IST. Afterward, τ_p remained at a level higher than that during the pre-sea-breeze period. In fact, the peak in τ_p is quite broad and τ_p did not show considerable decrease following the peak as on 21 February. Interestingly, prior to the occurrence of the main peak associated with the sea-breeze front, another minor peak occurred in τ_p at 0942 IST. This earlier peak appears to be associated with the breeze excursions during 0916–0958 IST seen in Fig. 5. On this day, low-level clouds formed after 1125 interrupting the MWR observations.

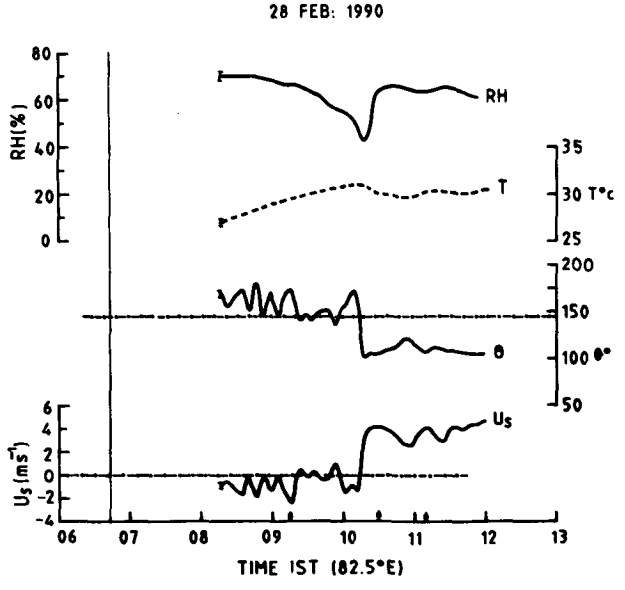

FIG. 5. Same as Fig. 1 but for 28 February 1990.

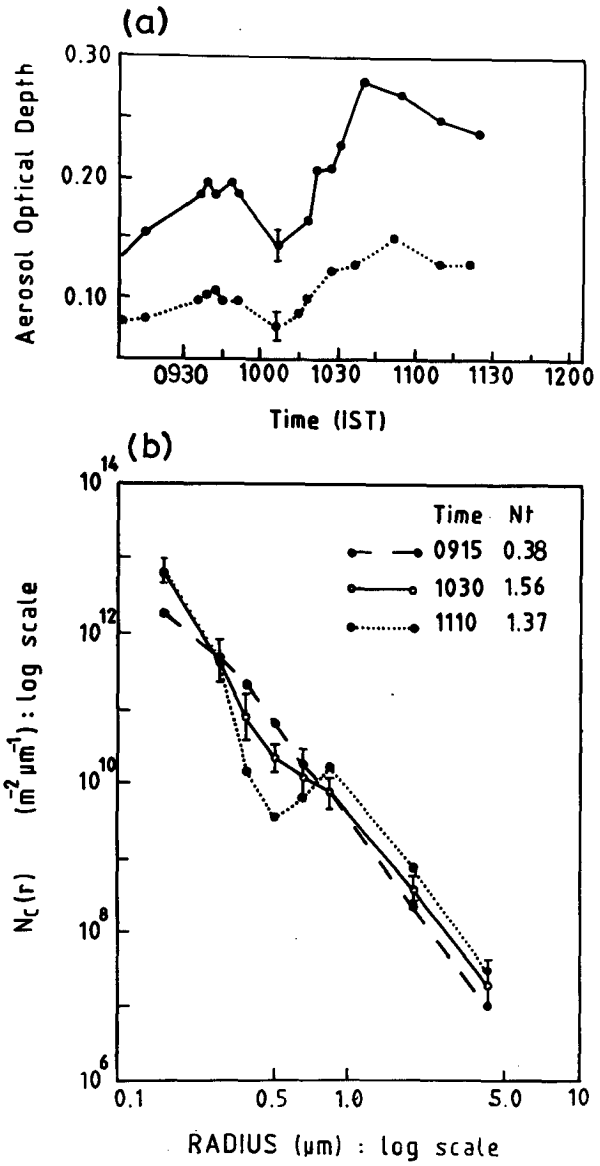

FIG. 6. Same as Fig. 2 but for 28 February 1990.

The SDs deduced from τ_p values at 0915, 1030, and 1110 IST are shown in Fig. 6b. The distribution changed from a near-inverse power-law form at 0915, to a bimodal form by 1110 IST. However, compared to SD at 0915, the SD at 1030 (close to the peak in τ_p) showed an increase in the small-particle ($r < 0.28$ μm) concentration and a decrease (though small) in the concentration of particles between 0.28 and 0.7 μm similar to the effect seen on 21 February frontal activity. However, it did not recover by 1110 as did the 21 February event; it instead showed a further de-

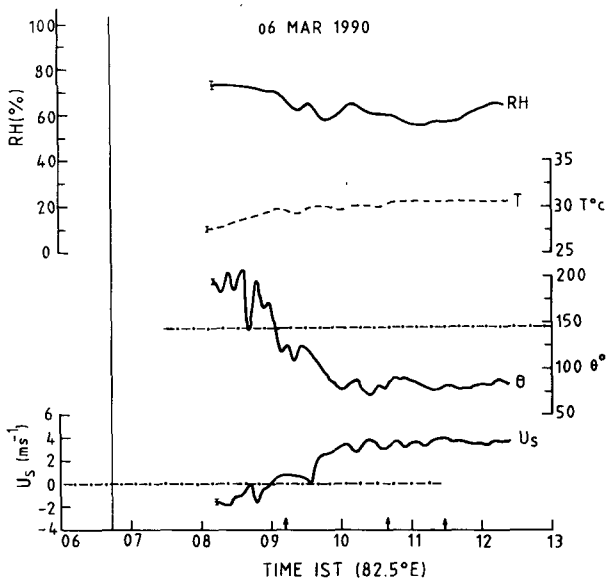

FIG. 7. Same as Fig. 1 but for 6 March 1990.

crease in the particle concentration in 0.28–0.7-μm range. There is also a small increase in the large-particle content (>1.0 μm) at 1110 compared to that at 0915 IST.

d. 6 March 1990

On this day, the sea breeze had set in quite early by approximately 0900 IST as seen from Fig. 7 and it took quite sometime for the sea breeze to stabilize in direction and magnitude (at 1000 IST). Relative humidity and temperature do not reveal any abrupt changes associated with the onset of sea breeze and so this day is considered a normal sea-breeze day in our analysis. Time variation of τ_p (Fig. 8a) resembles that of the 8 February event (Fig. 2a) and does not reveal any abrupt increase associated with the onset of sea breeze (However, small increases in τ_p are seen after the sea-breeze had stabilized). Figure 8b shows the SDs at 0915, 1040, and 1125 IST. All three SDs correspond to sea-breeze conditions except that the latter two are obtained after the sea breeze had stabilized. The SDs show transformation from a nearly inverse power-law type at 0915 to bimodal at 1040 with a tendency to recover by 1125 IST. There is a small decrease in concentration of particles between 0.28 and 0.62 μm from 0915 to 1040 and an increase in particle concentration with $r > 0.62$ μm with the stabilizing of sea breeze.

e. 7 March 1990

Variation of MET parameters (Fig. 9) shows an abrupt onset of sea breeze at 1010 IST. It also stabilized at a steady (nearly) direction (~100° azimuth) and magnitude quite rapidly. The signatures on RH and T seen in the figure around the onset time are similar to those seen on 21 February and 28 February and thus is also considered as a front event. Variations of τ_p at 450 and 750 nm depicted in Fig. 10a show features characteristic of those seen on the other two front days. The value of τ_p started increasing at about 1010 without any delay with respect to the onset of the sea breeze, attained its peak at about 1019, and decreased gradually afterward (reaching a low value by 1050 IST).

The SDs deduced from τ_p (Fig. 10b) show increase (though small) in particle concentration at sizes smaller than 0.62 μm and decrease at greater sizes associated with the onset of sea breeze and occurrence of peak in τ_p. Later, at 1130, the large-particle concentration appeared to recover to the prefront level whereas the small-particle concentration remained higher than the prefront level. Unlike on the other front days, the decrease in concentration during the front occurred from about 0.62 μm to 5 μm instead of in the midsize range (between approximately 0.28 and 0.62 μm). Also the

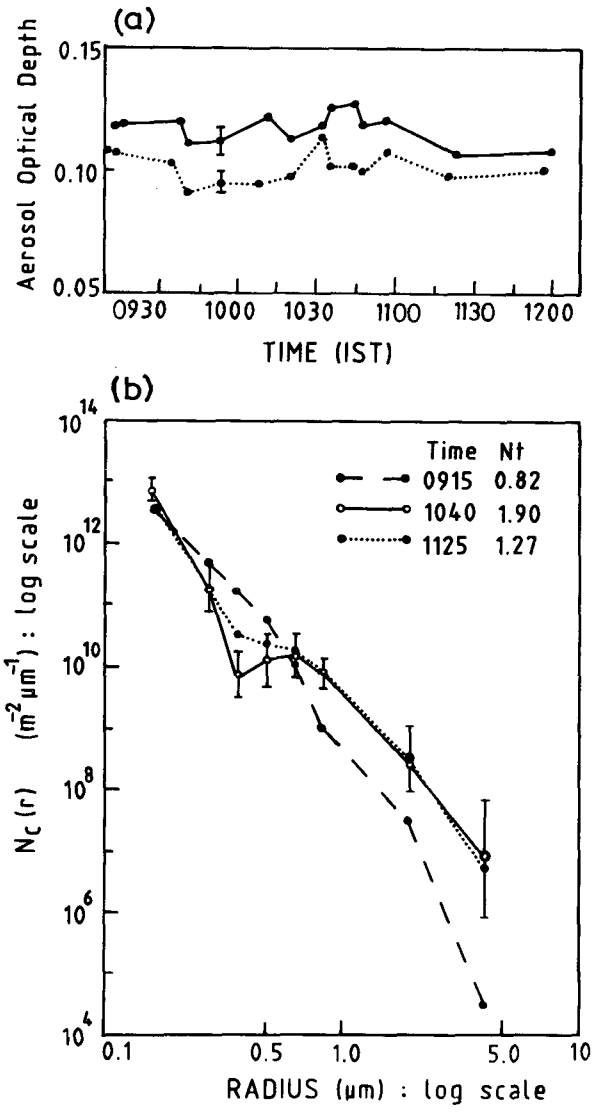

FIG. 8. Same as Fig. 2 but for 6 March 1990.

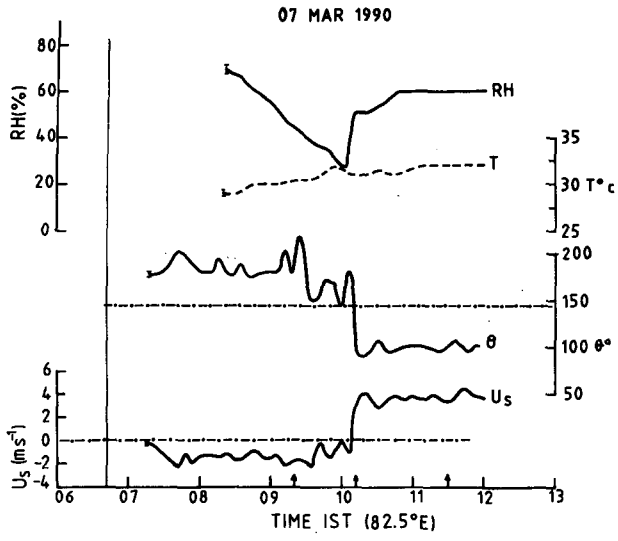

FIG. 9. Same as Fig. 1 but for 7 March 1990.

increase in small-particle concentration extended up to the size of 0.62 μm instead of up to 0.28 μm as in the earlier front days, but the increase and decrease are of very small magnitude.

f. 8 March 1990

On this day strong signature of the front is clearly discernible in RH and T (Fig. 11) around the rather late (at 1040 IST) seaward-to-landward reversal of the breeze. The change in wind direction has been somewhat gradual and the land breeze which prevailed in the morning prior to reversal had been quite strong with magnitudes of 3–4 m s^{-1}. The sea breeze also stabilized at higher values (5 m s^{-1}) even though the wind azimuth was about 100° as in the case of other front days. Relative humidity showed an abrupt increase from 30% at 1040 IST to more than 60% by 1058, and the ambient temperature dropped by as much as 2°C.

The temporal variations in τ_p, (shown in Fig. 12a at the two representative wavelengths), reveal an increase starting at 1040 IST and no perceptible delay with respect to the onset of sea breeze; τ_p reached its peak at 1055 and decreased to its prefront level by about 1110. The SD (shown in Fig. 12b), at 1050 (corresponding nearly to the occurrence time of peak τ_p) showed a remarkable change in shape to bimodal from the modified Junge-type prefront distribution. There is an increase in small-particle ($r < 0.28$ μm) concentration and a decrease in the concentration of particles between 0.28 and 0.62 μm compared to the prefront concentrations revealed by the distribution at 0930 IST. There is also significant increase in the concentration of (large) particles with sizes greater than 0.62 μm. The distribution then recovered to almost the same shape as the prefront SD shortly after the stabilizing of the sea breeze as evidenced by the SD at 1130 IST. Size distributions corresponding to pre- and postfront conditions are similar in nature (modified Junge-type) whereas the SD during the front is distinctly different from these and is bimodal type.

4. Discussion

We have investigated the behavior of aerosol optical depth on six days out of which four are considered "sea-breeze front" days with rapid changes in RH and T associated with onset of sea breeze. The other two days considered as "normal" sea breeze showed no such rapid changes. On all the front days the aerosol optical depth showed an abrupt increase followed by a decrease associated with the onset of sea breeze. Such changes are not observed on the normal sea-breeze days. It may be noted that the total aerosol optical depth as mea-

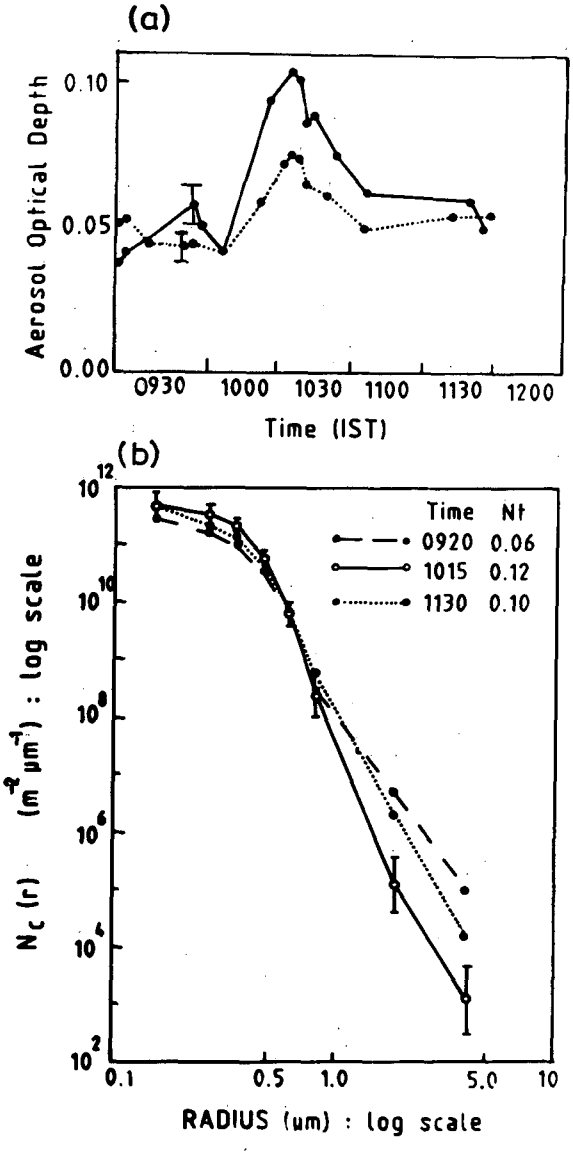

FIG. 10. Same as Fig. 2 but for 7 March 1990.

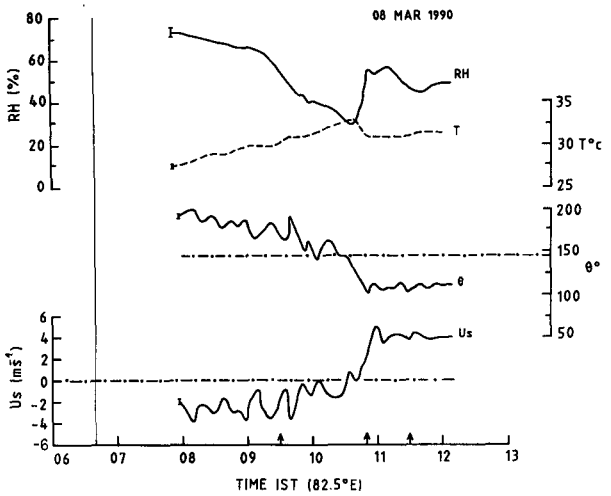

FIG. 11. Same as Fig. 1 but for 8 March 1990.

sured by the MWR is contributed mostly by the boundary-layer aerosols. Analysis of the total columnar aerosol size distributions obtained from the spectral aerosol optical depths, showed that the distributions exhibit, in general, more prominent bimodal nature during the time around the front passage compared to the SDs in the prefront period, except on one of the days (7 March), when no marked change in the distribution was seen associated with the front.

The total columnar content of aerosols in different ranges, deduced from the corresponding SDs are given in Table 1. An increase (above the error bars) can be seen in the concentration of small particles with $r < 0.28$ μm on all the days associated with the sea breeze. However, on the front days, this increase is quite significant except on 7 March 1990 where the increase is quite small, but extended up to 0.62 μm. The small particle content decreased later as the breeze stabilized (by 1110–1130 IST) even though these were still higher than the prefrontal values (except on the 8 March event). On all the front days there is a substantial decrease in the concentration of aerosols in the intermediate size range (0.28 μm to 0.62 or 0.7 μm) around the time of breeze reversal. On 21 February and 7 March this decrease extended to particle sizes up to or beyond approximately 2 μm also. On all these days (except 28 February) the aerosol content in this range recovered later (1110–1130 IST; close to the prefront values). On 28 February, however, an increase is seen in the content from 0.7 to 5.0 μm at 1110. (It may be noted that on this day low-level clouds formed at approximately 1125 IST and persisted for about an hour, interrupting the MWR observations). On the normal sea-breeze day of 8 February 1990, the aerosol content increased with time, with the increase in smaller-particle content being more significant. But on the other normal sea-breeze day, increase is seen both in the small and large particle ranges.

It is seen that sharp increases in RH (associated with the onset of sea breeze) occurred on all four days considered as front days in this analysis (Figs. 3, 5, 9, and 11). It is well established that significant increase in RH would cause growth of aerosols and leads to increased extinction (Hanel 1976; Shettle and Fenn 1979). This is particularly important in coastal environments where the aerosols (especially in the boundary layer) are likely to be hygroscopic. In order to estimate the contribution of changes in RH to the observed changes in τ_p associated with sea-breeze front activity, information on the altitude profile of RH in the boundary layer is required. However, such information is not available for the present study. As such, an approximate estimate of this has been made (for the period around the time of onset of sea breeze) as-

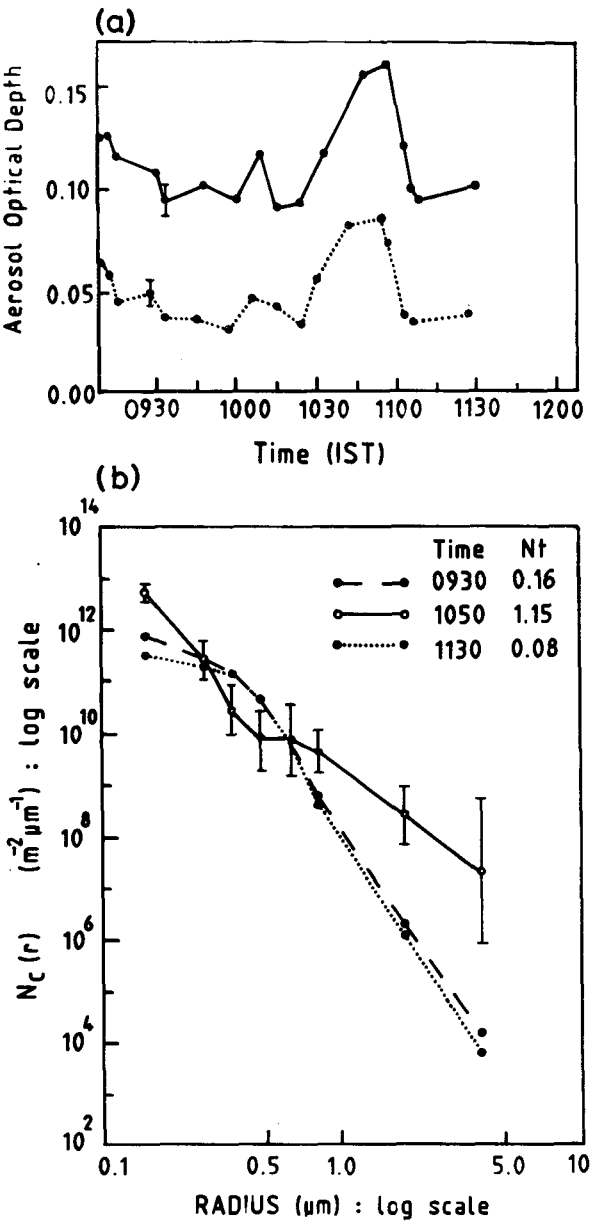

FIG. 12. Same as Fig. 2 but for 8 March 1990.

TABLE 1. Columnar aerosol content observed for various aerosol radii during field experiments.

Day	Range of r (μm)	Columnar aerosol content (10^{12} m^{-2})		
		0920 IST	1015 IST	1130 IST
8 February 1990	0.1–0.48	0.074	0.11	0.20
	0.48–5.0	0.006	0.01	0.01
	0.1–5.0	0.08	0.12	0.21
		0930 IST	1050 IST	1120 IST
21 February 1990	0.1–0.28	0.49	2.044	1.18
	0.28–5.0	0.01	0.003	0.01
	0.1–5.0	0.50	2.05	1.19
		0915 IST	1030 IST	1110 IST
28 February 1990	0.1–0.28	0.34	1.54	1.35
	0.28–0.7	0.04	0.02	0.01
	0.70–5.0	0.004	0.004	0.007
	0.1–5.0	0.38	1.56	1.37
		0915 IST	1040 IST	1125 IST
6 March 1990	0.1–0.28	0.75	1.87	1.24
	0.28–0.62	0.07	0.03	0.03
	0.62–5.0	0.001	0.004	0.005
	0.1–5.0	0.82	1.90	1.275
		0920 IST	1015 IST	1130 IST
7 March 1990	0.1–0.62	0.06	0.12	0.10
	0.62–5.0	0.0007	0.0005	0.0007
	0.1–5.0	0.06	0.12	0.10
		0930 IST	1050 IST	1130 IST
8 March 1990	0.1–0.28	0.13	1.14	0.05
	0.28–0.62	0.03	0.01	0.03
	0.62–5.0	0.001	0.003	0.001
	0.1–5.0	0.16	1.15	0.08

suming that an air parcel at ground level (along with the aerosols in it) is lifted adiabatically by the updrafts in the front and making use of the relevant equations (Kneizys et al. 1980). A mean (wet) adiabatic lapse rate of 6.5°C km^{-1} has been used based on meteorological pilot balloon data available at the station. The above estimate has been made for an altitude region of 0 to 1 km as this is the region that contributes most to the measured optical depth. The calculations reveal that an air parcel with RH of 55% at ground level when lifted adiabatically to 1 km will attain RH of 80% with RH values at the intermediate heights lying in between. Using the RH values thus obtained, the relative changes in integrated extinction (for 0–1 km) due to changes in the aerosol size and refractive index caused by changes in RH have been estimated using the data given by Shettle and Fenn (1979) for maritime aerosol models. This has been done for all four front days in this study, as the sharp changes in RH are observed only on these days. These estimates for the front days showed that the sharp increase in RH around the time of wind reversal can cause an increase in aerosol optical depth (integrated extinction) ranging from approximately 10% to 30%. However, the observed increases are in the range 30%–70%. Thus it appears that the sharp increase in RH associated with front could contribute significantly to the increase τ_p in the presence of updrafts, though it cannot totally account for the observed effects. On the normal sea-breeze days no sharp changes are seen either in RH or the wind direction associated with onset of sea breeze (to cause a strong updraft) and the aerosol optical depths also do not exhibit sharp increases. Also the increase in small particle concentration revealed by the SDs is small on these days.

Marine aerosols in the boundary layer are mainly due to local production whereas the marine free tropospheric aerosol distribution is governed by horizontal transport of aerosols from land areas and also transport (vertical) across the marine boundary layer (Patterson et al. 1980). The marine boundary-layer aerosols exhibit bimodal size distributions with a clear demarcation at $r = 0.5$ μm and are basically produced by two processes. The large particles ($r > 0.5$ μm) are produced by the bubble jet action and the smaller particles ($r < 0.5$ μm) by the breaking up of bubble film caps (Patterson et al. 1980). These primary production processes are related to the wind speed. In addition to these primary production processes there is also a small contribution from secondary production processes such as gas-to-particle conversion (Jaenicke 1984). On all the days of sea breeze studied in this investigation, small-particle content increased with the onset/stabilizing of the sea breeze, the increase being more prominent and abrupt on the front days compared to the normal days. Advection of aerosols over sea to land can contribute to this increase in small-particle content.

From the above discussion, it appears that the observed increase in the aerosol optical depth associated with the sea-breeze front can be attributed to two causes, namely, 1) increase in the concentration of aerosols especially in the small-particle range due to advection of aerosols over sea, and 2) growth of the particles due to abrupt increase in RH causing increase in optical depth. As pointed out earlier the lake- and sea-breeze fronts are characterized by a convergence zone with strong vertical updrafts (Keen and Lyons 1978; Ogawa et al. 1986; Prakash et al. 1992). These updrafts are confined to approximately 1 km above which is the return seaward flow giving rise to a downdraft behind the convergence zone to complete the flow circuit. This "convergence front cell" at times moves quite deep inland. In the return flow, in the downdraft region (behind the convergence zone) the aerosol particles are subjected to sedimentation and intermediate and large particles (as per the classification in this investigation) can be considered to be more efficiently removed by this process than the smaller particles (Lyons and Olsson 1973). As pointed out earlier, the marine aerosols (in the boundary layer) are, in general, bimodal with a clear demarcation around the 0.5-μm size, which corresponds to the intermediate size in the

present investigation. If the land aerosols do not have any such demarcation, as is the case for Trivandrum (Moorthy et al. 1991), then the land aerosols that are recycled will be deprived of their intermediate- and large-particle content (because of sedimentation). (On the seaward side of the convergence zone there could be no replenishment of fresh land aerosols.) In this situation, during the front passage, the aerosol content and SD are likely to exhibit a depletion in the intermediate size range (or even in the large-particle range) as observed in the present study. (An exception to this is on 8 March, when there is a large increase in the concentration of large particles ($r > 0.62$ μm) during the front passage.) The occurrence of these features will depend upon the relative concentrations of sea and land aerosols in different size ranges, the characteristics of the convergence zone, the movement of the front, the speed of the winds (particularly of sea breeze which influences the sea aerosols), and the subsidence. The decrease in τ_p (and in aerosol loading) subsequent to the passage of the front is obviously due to the inland movement of the convergence zone so that the solar ray path (in MWR observations) is through the clearer sea air behind the convergence front zone. In order to investigate these aspects further, aerosol observations need to be carried out at two or more stations inland and also over the sea along with the altitude profile of wind (at different times) preferably at two to three locations so that both spatial and temporal progression of the front with regard to effects on aerosols can be followed.

5. Conclusions

1) Aerosol optical depths (at a coastal station) show large increases associated with the sea-breeze fronts.

2) The small-particle content of aerosols appears to increase during the onset of sea breeze.

3) The increase in aerosol optical depth associated with sea-breeze front could be attributed to the combined effects of sharp increase in RH in the front convergence zone (updraft region) and to the increase in small-particle content due to advection of marine aerosols.

Acknowledgments. The authors are thankful to Dr. K. Narayanan Nair and other colleagues of the Boundary Layer Physics Branch of the Space Physics Laboratory for providing the required meteorological data and for useful discussions. The authors express thanks to the reviewers for their helpful comments.

REFERENCES

Bornstein, R. D., and W. T. Thompson, 1981: Effects of frictionally retarded sea-breeze and synoptic frontal passages on sulphur dioxide concentrations in New York City. *J. Appl. Meteor.*, **20,** 843–858.

Hanel, G., 1976: The properties of atmospheric aerosol particle as functions of relative humidity at thermodynamic equilibrium with the surrounding moist air. *Advances in Geophysics,* Vol. 19, H. E. Landsberg and J. Van Mieghem, Eds., Academic Press, 73–188.

Hunt, J. C. R., and J. E. Simpson, 1982: Atmospheric boundary layer over non-homogeneous terrain. *Engineering Meteorology,* E. J. Plate, Ed, Elsevier, 269–318.

Jaenicke, R., 1984: Physical aspects of atmospheric aerosol. *Aerosols and their Climatic Effects.* H. E. Gerber and A. Deepak, Eds., Deepak Publishing, 28 pp.

Keen, C. S., and W. A. Lyons, 1978: Lake/land breeze circulations on the western shore of Lake Michigan. *J. Appl. Meteor.*, **17,** 1843–1855.

King, M. D., 1982: Sensitivity of constrained linear inversions to the selection of Lagrange multiplier. *J. Atmos. Sci.*, **39,** 1356–1369.

Kneizys, F. X., E. P. Shettle, W. O. Gallery, J. H. Chitwynd, L. W. Abreu, J. E. A. Selby, R. W. Fenn, and R. A. McClatchey, 1980: Atmospheric transmittance/radiance: Computer code LOWTRAN 5.AFGL-TR-80-0067, Air Force Geophysics Laboratory, 217–219.

Leckner, B., 1978: The spectral distribution of solar radiation at the earth's surface-elements of a model. *Sol. Energy,* **20,** 143–150.

Lyons, W. A., and L. E. Olsson, 1973: Detailed mesometeorological studies of air pollution dispersion in the Chicago lake breeze. *Mon. Wea. Rev.*, **101,** 387–403.

McClatchey, R. A., R. W. Fenn, J. E. A. Selby, F. E. Volz, and S. Garing, 1972: Optical properties of the atmosphere. Report, AFCRL-72-997, Air Force Cambridge Research Laboratories, Bedford, MA.

Moorthy, K. K., P. R. Nair, and B. V. Krishna Murthy, 1989: Multiwavelength solar radiometer network and features of aerosol spectral optical depth at Trivandrum. Ind. *J. Radio & Space Phys.*, **18,** 194–201.

——, ——, and ——, 1991: Size distribution of coastal aerosols: Effects of local sources and sinks. *J. Appl. Meteor.*, **30,** 844–852.

Nair, S., and V. Narayanan, 1980: Diurnal variation of lower tropospheric winds (0–3 km) over Thumba during 18–20 August 1976. *Mausam,* **31,** 409–414.

Narayanan, V., 1967: An observational study of the sea breeze at an equatorial coastal station. *Ind. J. Meteor. and Geophys.*, **18,** 497–504.

Ogawa, Y., T. Ohara, S. Wakamatsu, P. G. Diosey, and I. Uno, 1986: Observation of lake breeze penetration and subsequent development of the thermal internal boundary layer for the Nanticoke II shoreline diffusion experiment. *Bound.-Layer Meteor.*, **35,** 207–230.

Parvanov, O., I. Kolev, B. Kaprielov, V. Polianov, and G. Korchev, 1988: Lidar observation of aerosol structure in the marine planetary boundary layer. Abstracts, *Fourteenth Int. Laser Radar Conf.,* Innichen-San Candido, Italy, ICLAS/IRC/IAMAP, 49–52.

Patterson, E. M., C. S. Kiang, A. C. Delany, A. F. Wartburg, A. C. D. Lesli, and B. J. Huebert, 1980: Global measurements of aerosols in remote continental and marine regions: Concentrations, size distributions, and optical properties. *J. Geophys. Res.*, **85,** 7361–7376.

Prakash, J. W. J., R. Ramachandran, K. N. Nair, K. S. Gupta, and P. K. Kunhikrishnan, 1992: On the structure of sea-breeze fronts observed near the coastline of Thumba, India. *Bound.-Layer Meteor.*, **59,** 111–124.

Sasi, M. N., and K. Sen Gupta, 1979: A model equatorial atmosphere over the Indian zone from 0 to 80 km. Report, ISRO:VSSC: SR:19:79, Indian Space Research Organisation, Bangalore, 39 pp.

Shaw, G. E., J. A. Reagan, and B. M. Herman, 1973: Investigations of atmospheric extinction using direct solar radiation measurements made with a multiple wavelength radiometer. *J. Appl. Meteor.*, **12,** 374–380.

Shettle, E. P., and R. W. Fenn, 1979: Models for the aerosols of the lower atmosphere and the effects of humidity variations on their optical properties. AFGL-TR-079-0214, Air Force Geophysical Laboratory, MA 01731, 94 pp.

Simpson, J. E., D. A. Mansfield, and J. R. Milford, 1977: Inland penetration of sea breeze fronts. *Quart. J. Roy. Meteor. Soc.*, **103,** 46–76.